Comments to the Editor

Response to Comment on Article: Hydrodynamics of Sperm Cells Near Surfaces

ABSTRACT In the Comments to a recent study by Elgeti, Kaupp, and Gompper, the authors state that we attributed differences between our study and a previous study by Smith et al. to methodological flaws in the latter article. This interpretation is unwarranted. However, the authors raise the interesting possibility that species-specific details of cell morphology might account for the different predictions concerning the distance *d* of adhering sperm from the surface. We present new simulation results, which show that the density distribution as a function of *d* strongly depends on midpiece curvature and head size.

INTRODUCTION

The swimming behavior of sperm is an important aspect of reproduction. In pioneering experiments, Rothschild (1) showed that sperm accumulate near surfaces. In past years, numerical methods to simulate hydrodynamic flow have been used to study swimming of sperm near surfaces. We used multiparticle collision dynamics, a particle-based mesoscale simulation technique, to study sperm accumulation near surfaces (2) (referred to in this Comment as Elgeti, Kaupp, and Gompper). Sperm adhesion is due to a combination of hydrodynamic attraction caused by a dipolar flow field, a steric interaction due to the rodlike average shape of sperm, and a small tilt of the sperm axis toward the surface. The result is qualitatively consistent with the hydrodynamic attraction obtained by a far-field approximation (3), and the accumulation of rodlike Brownian swimmers near surfaces (4,5).

These predictions also agree qualitatively with a study based on a Stokes-flow simulation (6) (referred to in this Comment as Smith et al.). However, there are important quantitative differences between Elgeti, Kaupp, and Gompper and Smith et al.:

1. Sperm swim close to the surface in Elgeti, Kaupp, and Gompper, yet swim at a finite distance of 15–60% of the sperm length in Smith et al.
2. The sperm axis is slightly tilted toward the surface in Elgeti, Kaupp, and Gompper, but tilted away from the surface in Smith et al.

Elgeti, Kaupp, and Gompper suggested two possible explanations for these differences. First, Smith et al. found that for "…initial (inclination) angles of 0–2°, the cell performs an oscillatory trajectory…" converging to a stationary state at a fixed distance from the surface, while "…for angles of 4–6°, the cell 'rebounds' from the surface and escapes." This led Elgeti, Kaupp, and Gompper to conclude that the adhering state is "marginally stable" and, therefore, this state might be susceptible to fluctuations in sperm orientation. We meant, and should have written more precisely, weakly stable. Second, Smith et al. stated that "…for angles of 8° or greater, the cell is predicted to collide with the surface, before which point the current modeling framework is no longer valid." We referred to this as "numerically unstable" but did not intend to suggest a methodological flaw in the numerical approach of Smith et al. In any case, this inherent limitation prevented Smith et al. from studying trajectories very close to the surface.

In their Comment, Smith, Gaffney, Shum, Gadêlha, and Kirkmann-Brown (denoted Smith, Gaffney et al. below) emphasize two new and important aspects:

1. The shape and size of the sperm head, which is different in Elgeti, Kaupp, and Gompper and Smith et al., might play an important role.
2. Experiments of Winet et al. (7) show a broad distance distribution, perhaps with a dip of ~30% near the surface.

ACCURACY OF MESOSCALE HYDRODYNAMICS NEAR SURFACES

We completely agree with Smith, Gaffney et al. that any accurate simulation of the very close interaction of a solid body with a surface in Stokes flow is difficult, both for continuum dynamics models and for mesoscale simulation techniques. To verify the hydrodynamic interaction of the flagellum beating near a planar wall, we have considered a rod which is dragged parallel to a wall at a constant distance h, with the force perpendicular to the rod orientation. For this situation, analytical results within the Stokes approximation are available (8). For a rod of radius r pulled at constant velocity U, the drag force F_x per unit length is (8)

$$F_x/L = -4\pi\eta U/\ln\left[\left\{h + \left(h^2 - r^2\right)^{1/2}\right\}\Big/ r\right]. \quad (1)$$

This equation applies for rod lengths L much larger than h. The simulation results for the drag force F_x/L—extrapolated

Submitted December 23, 2010, and accepted for publication March 16, 2011.

*Correspondence: g.gompper@fz-juelich.de

0006-3495/11/05/2321/4 $2.00

doi: 10.1016/j.bpj.2011.03.016

to infinite system size—as a function of the distance from the wall are shown in Fig. 1. Excellent agreement with Eq. 1 is obtained for $h \gtrsim 2a$, without any adjustable parameters (where a is the size of the collision box in multiparticle collision dynamics, the minimal length of hydrodynamic resolution). For smaller distances, the friction coefficient $F_x/(UL)$ obtained from simulations increases less strongly than the logarithmic divergence predicted by Eq. 1, but still captures qualitatively the further increase with decreasing h. For further details, see the Supporting Material of Elgeti, Kaupp, and Gompper.

In the simulations of Elgeti, Kaupp, and Gompper, the average distance of the flagellum to the wall is ~$3a$, and the flagellum rarely comes closer to the wall than $1.5a$. We conclude that our simulation represents near-wall hydrodynamics quantitatively.

As a further indication of the suitability of multiparticle collision dynamics to study the hydrodynamics of active swimmers, we want to mention the calculation of the velocity of sinusoidally beating flagella in a two-dimensional fluid in Yang et al. (9). In this case, analytical results for the velocity v of an infinitely long flagellum at Reynolds number $Re = 0$ are available (10), with

$$v = \frac{\omega A_{fl}^2}{\lambda}\left(1 - \frac{19\pi^2}{4}\frac{A_{fl}^2}{\lambda^2}\right), \qquad (2)$$

where λ is the wavelength, ω the beat frequency, and A_{fl} the beat amplitude of the sinusoidal wave on the flagellum. With the parameters used in the simulations of Yang et al. (9), a velocity v is obtained from Eq. 2, which deviates $<10\%$ from the simulation result; the small difference can probably be attributed to end effects, because the wavelength λ equals the flagellum length in the simulation model. This demonstrates that the simulation model fairly well describes the limit of low-Reynolds-number hydrodynamics of active swimmers.

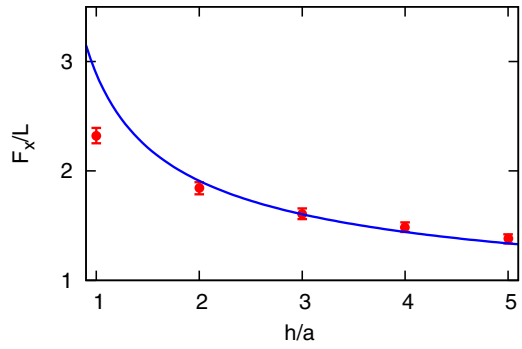

FIGURE 1 (*Color online*) Drag force F_x/L per unit length (in units of k_BT/a^2), for velocity $U = 0.02\sqrt{k_BT/m}$, as a function of the distance h from a plane wall with no-slip boundary conditions (where k_BT is the thermal energy and m is the fluid-particle mass). Symbols (*red*) indicate simulation results obtained from finite size scaling; the solid (*blue*) line shows the theoretical expression (1) without any adjustable parameters.

EXPERIMENTAL EVIDENCE

Smith, Gaffney et al. state that the experiments of Winet et al. (7) "… provide ample evidence that the predictions of Smith et al. are consistent with physical reality." It is therefore worthwhile to take a closer look at the experimental results. Winet et al. (7) study human sperm (with a total length of ~50 μm) in an observation chamber with two parallel walls at a distance $D = 310$ μm. The depth of field for the microscope objective used was 4 μm. The analysis was restricted to those spermatozoa that remained in the plane of focus (parallel to the wall) for at least 0.625 s and were swimming on nearly straight trajectories with a velocity of at least 30 μm/s, i.e., covered 18 μm. The results of Winet et al. (7) are reproduced in Fig. 2. The data shows a smoothly decaying density distribution, which essentially vanishes at a distance of ~50 μm, and which has a small dip at the surface.

To our knowledge, no other study since Winet et al. (7) provides information on the distance of sperm from the wall. Clearly, further experiments are needed to clarify this issue.

DENSITY DISTRIBUTIONS, HEAD SIZE, AND IMPORTANCE OF FLUCTUATIONS

The trajectories of MCS sperm—the sperm model of Elgeti, Kaupp, and Gompper with curved midpiece and straight tail of high torsional stiffness—shown in Fig. 8 of Elgeti, Kaupp, and Gompper (2) demonstrate that sperm adhesion strongly depends on the preferred midpiece curvature $c_0^{(m)}$. The corresponding probability-density distributions in Fig. 3 illustrate that sperm are highly localized to the surface for large $c_0^{(m)}$, but are only weakly adhering to the surface for small (although nonzero) $c_0^{(m)}$. The broad distribution is due to the rolling movement of sperm and to sperm moving back and forth between walls. The distribution is qualitatively similar to the experimental distributions of

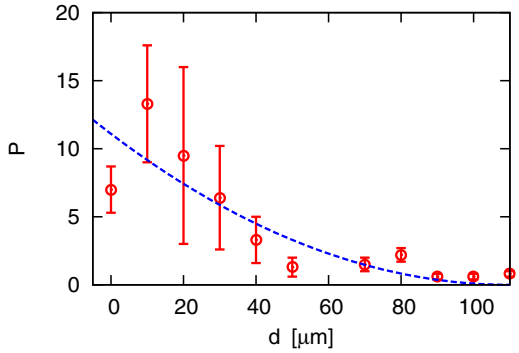

FIGURE 2 (*Color online*) Density distribution P (not normalized) of human sperm as a function of distance d from the wall (7). The total number of sperm in the sample is 345. Values with error bars represent 2–5 samples. The direction of the gravitational field is parallel to the walls. The dashed (*blue*) line is a guide to the eye. Redrawn from Fig. 6 of Winet et al. (7).

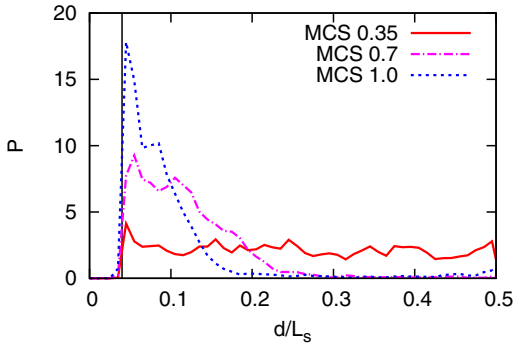

FIGURE 3 (*Color online*) Probability-density distribution P (of center-of-mass position of sperm head) of simulated MCS sperm with curved midpiece, as a function of distance d from the wall (in units of the sperm length L_s). Data are shown for midpiece curvatures $c_0^{(m)} = 0.35\ L_m^{-1}$ (*solid/red line*), $c_0^{(m)} = 0.7\ L_m^{-1}$ (*dashed-dotted/purple line*), and $c_0^{(m)} = 1.0\ L_m^{-1}$ (*dotted/blue line*), where L_m is the midpiece length. The wavelength of the tail undulations is $\lambda = 2L_t/3$, where L_t is the length of the active part of the flagellum. The vertical (*black*) line indicates the minimal distance from the wall due to the head size ($r_h = 2.0a$). Note that the wall separation D equals the sperm length $L_s = 50a$, and, therefore, is much smaller than in the experiments of Winet et al. (7).

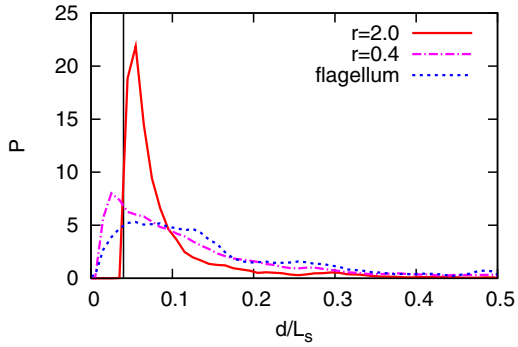

FIGURE 4 (*Color online*) Probability-density distribution P (of center-of-mass position of sperm head) of simulated MCS sperm with symmetric average shape, as a function of distance d from the wall (in units of the sperm length L_s). Data are shown for large head radius $r_h = 2.0a$ (*solid/red line*), small head radius $r_h = 0.4a$ (*dashed-dotted/purple line*), and a flagellum—without head and midpiece (*dotted/blue line*). All other parameters are the same as employed in Elgeti, Kaupp, and Gompper (2). The wall separation D equals the sperm length. Differences between the probability distributions of different runs for the same model indicate a statistical error of ~5% for sperm with large head, and ~15% for both sperm with small head and for the flagellum alone.

human sperm (7). It should be noted that the investigation of Winet et al. (7) focused on nearly straight trajectories (i.e., sperm with very small preferred curvature), and that the wall separation D in the simulations (corresponding to ~50 μm) is much smaller than in the experiments.

Smith, Gaffney et al. raise an important question regarding the effect of head size, head shape, and beat frequency. Therefore, we have investigated the effect of head size on the density distribution by our mesoscale simulation approach, and present some preliminary data here for symmetric sperm (K. Marx, Y. Yang, J. Elgeti, U. B. Kaupp, and G. Gompper, unpublished). Sperm adhesion to surfaces is expected to decrease for smaller head size, because the hydrodynamic dipole strength gets reduced, and thereby the hydrodynamic attraction; furthermore, the steric adhesion effect is expected to decrease with decreasing swimming velocity. Indeed, for symmetric sperm, with approximately linear trajectories, the simulation data in Fig. 4 clearly show a broadening of the distribution; for the smaller head size, the simulated distributions strongly resemble the experimental results in Fig. 2. The hydrodynamic dipole strength and the adhesion is reduced further by removing the passive midpiece (see Fig. 4), which in the MCS model has a length of 10% of the flagellum.

To obtain the probability distribution of sperm as a function of distance d from the wall, simulations equivalent to those in Elgeti, Kaupp, and Gompper are performed. Single sperm are initially placed at distances $d_0 = D/8$, $D/4$, or $D/2$ from the wall, with orientation parallel to the wall (where D is the separation of the two wall). The only difference to the MCS model of Elgeti, Kaupp, and Gompper lies in the sperm structure. For the smaller head radius (20% of the radius used by Elgeti, Kaupp, and Gompper) only $N_h = 12$ monomers (instead of $N_h = 163$ monomers for the bigger head) are used. For the flagellum simulations, the head is removed completely, and the whole flagellum beats actively. The probability distributions in Fig. 4 are then calculated as time and ensemble averages over single sperm trajectories, where three independent runs are performed for each parameter set and initial condition (with each run extending over thousands of beats).

It is important to emphasize that such a broad distribution of wall distances results from fluctuations. Such fluctuations can be due to thermal noise or biochemical noise in the beat pattern (11).

CONCLUSIONS

We agree with Smith, Gaffney et al. that the head size and head shape are important parameters for a quantitative understanding of the swimming pattern and density distribution of sperm. We have shown that, in our model, the probability-density distribution of symmetric sperm broadens with decreasing head size.

However, some questions remain. First, the differences in the results of Elgeti, Kaupp, and Gompper and Smith et al. still need an explanation. It should be possible to study the effect of head shape and head tilt angle on the sperm distance from the wall by the Smith et al. model, because such head shapes have already been implemented (12). Second, is the experimentally observed density distribution due to an ensemble average over many sperm cells, each of which beats and swims differently? In our opinion, this seems to be the only explanation of how the Smith et al.

model can achieve a broad distribution. Or is the broad distribution due to fluctuations or small preferred curvatures, and thus rolling, of individual sperm, as the Elgeti, Kaupp, and Gompper model suggests? We trust that precise measurements of the trajectory of sperm with different morphology swimming along a surface will shed light on this old and interesting phenomenon.

Jens Elgeti,[†‡] U. Benjamin Kaupp,[§] and Gerhard Gompper[†*]

[†]*Institute of Complex Systems, Forschungszentrum Jülich, Jülich, Germany;*
[‡]*Institut Curie, Centre National de la Recherche Scientifique, UMR 168, Université Pierre et Marie Curie, Paris, France; and*
[§]*Center of Advanced European Studies and Research (CAESAR), Bonn, Germany*

REFERENCES

1. Rothschild, L. 1963. Non-random distribution of bull spermatozoa in a drop of sperm suspension. *Nature.* 198:1221–1222.
2. Elgeti, J., U. B. Kaupp, and G. Gompper. 2010. Hydrodynamics of sperm cells near surfaces. *Biophys. J.* 99:1018–1026.
3. Berke, A. P., L. Turner, …, E. Lauga. 2008. Hydrodynamic attraction of swimming microorganisms by surfaces. *Phys. Rev. Lett.* 101:038102.
4. Elgeti, J., and G. Gompper. 2009. Self-propelled rods near surfaces. *EPL.* 85:38002.
5. Li, G., and J. X. Tang. 2009. Accumulation of microswimmers near a surface mediated by collision and rotational Brownian motion. *Phys. Rev. Lett.* 103:078101.
6. Smith, D. J., E. A. Gaffney, …, J. C. Kirkman-Brown. 2009. Human sperm accumulation near surfaces: a simulation study. *J. Fluid Mech.* 621:289–320.
7. Winet, H., G. S. Bernstein, and J. Head. 1984. Observations on the response of human spermatozoa to gravity, boundaries and fluid shear. *J. Reprod. Fertil.* 70:511–523.
8. Jeffrey, D. J., and Y. Onishi. 1981. The slow motion of a cylinder next to a plane wall. *Q. J. Mech. Appl. Math.* 34:129–137.
9. Yang, Y., V. Marceau, and G. Gompper. 2010. Swarm behavior of self-propelled rods and swimming flagella. *Phys. Rev. E.* 82:031904.
10. Taylor, G. I. 1951. Analysis of the swimming of microscopic organisms. *Proc. R. Soc. Lond. A Math. Phys. Sci.* 209:447–461.
11. Friedrich, B. M., and F. Jülicher. 2009. Steering chiral swimmers along noisy helical paths. *Phys. Rev. Lett.* 103:068102.
12. Gadêlha, H., E. A. Gaffney, …, J. C. Kirkman-Brown. 2010. Nonlinear instability in flagellar dynamics: a novel modulation mechanism in sperm migration? *J. R. Soc. Interface.* 7:1689–1697.